

# Journal of Biomedical Optics

[SPIDigitalLibrary.org/jbo](http://SPIDigitalLibrary.org/jbo)

## **Rapid confocal imaging of large areas of excised tissue with strip mosaicing**

Sanjee Abeytunge  
Yongbiao Li  
Bjorg Larson  
Ricardo Toledo-Crow  
Milind Rajadhyaksha

# Rapid confocal imaging of large areas of excised tissue with strip mosaicing

Sanjee Abeytunge,<sup>a</sup> Yongbiao Li,<sup>a</sup> Bjorg Larson,<sup>b</sup> Ricardo Toledo-Crow,<sup>a</sup> and Milind Rajadhyaksha<sup>b</sup>

<sup>a</sup>Memorial Sloan-Kettering Cancer Center, Research Engineering Laboratory, 430 East 67th Street, RRL513, New York, New York 10065

<sup>b</sup>Memorial Sloan-Kettering Cancer Center, Dermatology Service, 160 East 53rd Street, 2nd floor, New York, New York 10022

**Abstract.** Imaging large areas of tissue rapidly and with high resolution may enable rapid pathology at the bedside. The limited field of view of high-resolution microscopes requires the merging of multiple images that are taken sequentially to cover a large area. This merging or mosaicing of images requires long acquisition and processing times, and produces artifacts. To reduce both time and artifacts, we developed a mosaicing method on a confocal microscope that images morphology in large areas of excised tissue with sub-cellular detail. By acquiring image strips with aspect ratios of 10:1 and higher (instead of the standard ~1:1) and “stitching” them in software, our method images  $10 \times 10 \text{ mm}^2$  area of tissue in about 3 min. This method, which we call “strip mosaicing,” is currently three times as fast as our previous method. © 2011 Society of Photo-Optical Instrumentation Engineers (SPIE). [DOI: 10.1117/1.3582335]

**Keywords:** Mohs surgery; confocal fluorescence mosaicing microscopy; basal cell carcinoma; surgical pathology; large area imaging microscopy.

Paper 11027LR received Jan. 14, 2011; revised manuscript received Apr. 4, 2011; accepted for publication Apr. 4, 2011; published online May 26, 2011.

In surgical oncology, the selective excision of tumors with minimal damage to the surrounding normal tissue is critical. Tumor removal is guided by examining pathology that is prepared during surgery from the excisions. Preparation of pathology is labor intensive and time consuming. Typical preparation time is hours for frozen pathology during Mohs surgery and days for fixed pathology in other surgical settings such as head-and-neck and breast.<sup>1</sup> This often results in insufficient sampling of tissue and incomplete removal of a tumor such that 20% to 70% of the patients must subsequently undergo further resection, radiotherapy and/or chemotherapy.<sup>2,3</sup> Confocal mosaicing microscopy potentially offers an approach for detecting cancer margins rapidly and with the necessary sub-cellular resolution.<sup>1,4</sup> In this process, merging individual images creates mosaics that display large areas of tissue. The feasibility of imaging<sup>5</sup> and mosaicing<sup>6</sup> skin cancer margins *in vivo* in reflectance contrast has been demonstrated. More recently, feasibility for mosaicing

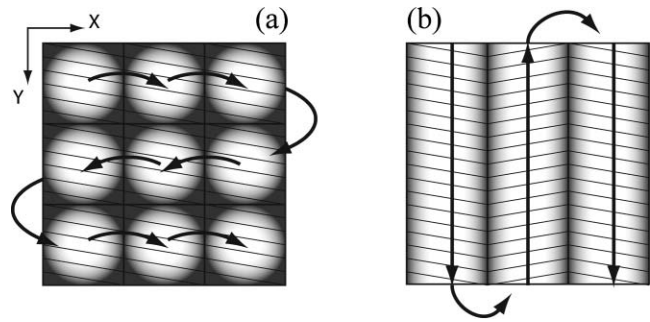


**Fig. 1** (a) A two-dimensional mosaic acquisition pattern. The individual images have radial illumination falloff (as shown in the diagram) that must be corrected and each image must be “stitched” to two neighbors (on average). (b) In strip mosaicing the optics acquire a single line in the X direction while a stage scans the sample in the Y direction (straight arrows). The intensity fall-off is in the horizontal direction only and each image must be stitched to a single neighbor.

in endoscopy and intraorally was reported.<sup>7,8</sup> However, at present, mosaicing *in vivo* has been demonstrated either on relatively small areas ( $\sim \text{mm}^2$ ) or along linear paths ( $\sim \text{mm}$ ) with long acquisition times ( $\sim$ minutes), whereas surgeons need to examine much larger areas ( $\sim \text{cm}^2$ ) in shorter times ( $\sim 1$  min). To address these issues, we designed a new method called strip-mosaicing.

We previously reported a confocal mosaicing microscope that images a  $12 \times 12 \text{ mm}^2$  area of Mohs surgical excisions by acquiring  $36 \times 36$  images and merging them with custom software.<sup>9,10</sup> Fluorescence contrast using acridine orange to stain nuclei was shown to be superior to reflectance contrast for the detection of basal cell carcinomas. In a blinded examination of 45 fluorescence mosaics by two Mohs surgeons, basal cell carcinomas were detected with sensitivity of 96.6% and specificity of 89.2%. The time for image acquisition and two-dimensional mosaicing was 9 min. While this showed initial feasibility, the acquisition and stitching time required for larger excisions ( $\sim \text{cm}^2$ ) that are routinely taken in other surgical settings make this impracticable.

In this report, we eliminate one of the stitching dimensions by acquiring long image strips instead of the standard “square” images. Instead of merging a two-dimensional array of images, a single one-dimensional array of strips is stitched together (see Fig. 1). The benefit of this is threefold: the acquisition time, merging time, and the artifacts due to the illumination variations are all reduced by half. The system described uses a combination of optical and mechanical scanning to generate the images. Preliminary data shows that the system can produce a  $10 \times 10 \text{ mm}^2$  strip mosaic in about 3 min.

Our system is based on a point-scanning confocal microscope with a rotating polygonal mirror and a galvanometrically driven mirror (Vivascope 2000, Lucid Inc.)<sup>9,10</sup> A laser (Ar + 488 nm) is scanned in the fast (X) direction at 6.8 kHz over  $408 \mu\text{m}$  at the sample through a  $30 \times 0.9 \text{ NA}$ , water immersion objective lens (Stableview, Lucid Inc.) The captured field of view is  $330 \mu\text{m}$  to limit the intensity falloff at the edges of the scan. The fluorescence signal is captured with a digital acquisition card (DAQ PCI-6110, National Instruments). A custom

Address all correspondence to: Ricardo Toledo-Crow, Memorial Sloan-Kettering Cancer Center, Research Engineering Laboratory, 1275 York Ave, Box 137, New York, NY 10065. Tel: 212-639-8048; Fax: 212-717-3604; E-mail: toledocr@mskcc.org.

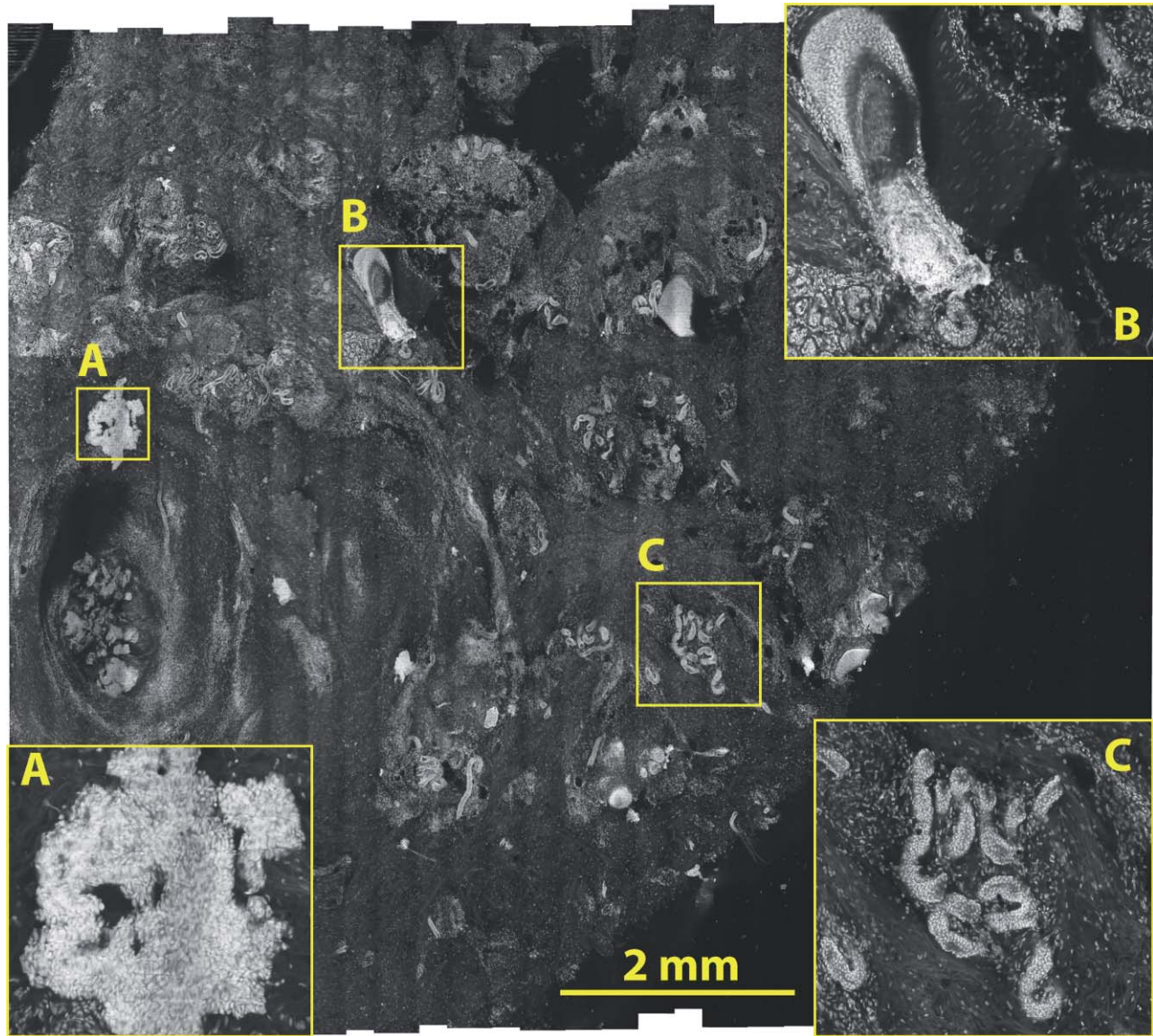


**Fig. 2** A  $10 \times 10$  mm<sup>2</sup> mosaic consisting of 31 fluorescence image strips of excised tissue from Mohs surgery. The tissue was stained with 0.6 mM acridine orange for 20 s (Refs. 9 and 10). Nests of basal cell carcinomas (A) are observed, showing nuclear detail such as increased density, pleomorphism, and palisading. Typical normal features such as hair follicles and sebaceous glands (B) and eccrine ducts (C) can be seen. The mosaic dimensions are 11,415  $\times$  10,291 (pixels wide  $\times$  high) with 8 bits/pixel. Note that the magnified areas are digital zooms obtained from the original image showing the detail and resolution of the mosaic. The features in the mosaic compare well to the pathology (Fig. 3), in terms of location, shape, size, nuclear detail and overall morphology of both basal cell carcinomas and normal features.

tissue fixture is used for mounting large skin excisions from Mohs surgery with precise orientation and alignment to the objective lens.<sup>11</sup> It provides tip-tilt adjustments of the glass slide and samples relative to the objective lens to make the imaging and scanning planes parallel, ensuring that the data is captured at a constant depth from the glass-tissue interface.

The theoretical lateral and axial resolutions, as per the Rayleigh criteria, are 0.33  $\mu$ m radially (Airy radius) and 1.61- $\mu$ m axially, assuming a planar wave and a circular aperture. We approximate this by overfilling the back aperture of the objective lens and using the central portion of the Gaussian beam. The Rayleigh criterion requires sampling at half the Airy radius. To increase the scanning speed we undersample the data by a factor of  $\sim 6$  which results in a  $\sim 1$   $\mu$ m pixel size.

As reported in our earlier studies<sup>9,10</sup> the undersampled images are adequate for interpretation by surgeons and pathologists. To obtain square pixels and equal spatial sampling rates in X and Y, the stage speed must be  $\sim 6.8$  mm/s (1  $\mu$ m pixel  $\times$  6.8 kHz line rate). Thus, it takes  $\sim 1.5$  s to scan a 10 mm strip plus 0.5 s to move the stage laterally before starting to acquire the adjacent strip. This is about 2 s/strip. A 31 strip ( $\sim 10$ -mm wide) mosaic takes approximately 1 min to capture.

To acquire a strip image the galvanometric mirror is locked to its center position and the fast (X) scanner is started. The Y stage motor is started and monitored by a hardware counter. On reaching a constant speed after  $N$  steps, the DAQ starts acquiring image lines on the next valid horizontal line trigger from the scanner. This ensures that the strips do not have more than

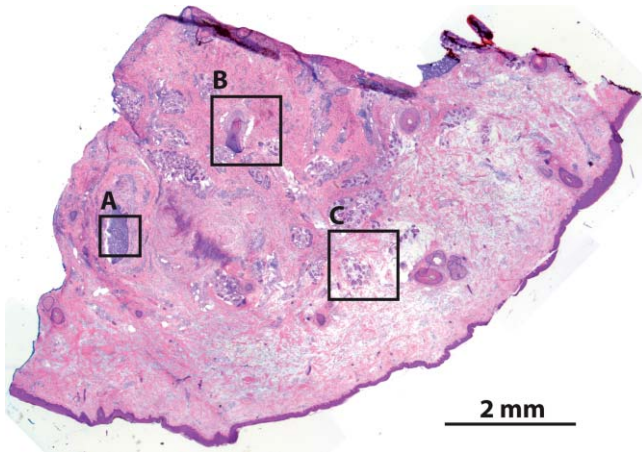


**Fig. 3** Frozen H&E-stained pathology of excised tissue from Mohs surgery. The wide-field microscopy images correspond to a tissue slice adjacent to the one shown in Fig. 2. The features corresponding to areas A, B, and C can be identified across the two figures.

a single line of misalignment.  $M$  lines are acquired and then the stage is stopped. The  $X$  stage motor moves the sample laterally by  $330\ \mu\text{m}$  (80% of the imaged field) and the process starts anew. Thirty-one strips were acquired in the example shown in this paper (Fig. 2). After completing the acquisition, the images are loaded into the MosaicJ open source mosaicing software,<sup>12</sup> together with information on their relative positions. The program automatically places the images in their acquired positions and merges the images with corrections for any remnant misalignments and variations in signal level. The merging time depends on the power of the processing computer. On an Mac Pro ( $2\times 2.93\ \text{GHz}$  Quad-Core Xeon, 16 GB RAM) it took 35 s to load 31 images and 92 s of processing by MosaicJ to form Fig. 2. Although our system is designed to accurately synchronize the scanner and stage to acquire strip images that are adjacent to each other with a vertical misalignment of no more than one line, there remain some misalignments that are entirely due to inadequate precision in our stages. This, of course, can be easily corrected with newer and better quality hardware.

Figure 2 shows a strip mosaic of a skin excision from Mohs surgery. The total time for acquisition and merging of the 31 image strips was about 3.1 min. The mosaic shown is in fluorescence contrast. Acridine orange was used to stain because its excitation matches the 488-nm wavelength in our system. Any contrast agent can be used, such as methylene blue,<sup>4</sup> with a suitable excitation source. The mosaic shows the morphology of a basal cell carcinoma and typical normal features (Fig. 2). The nuclear morphology is not readily visible in small figures but is clearly seen on a large monitor. To show the detail as seen on a monitor, we present the magnified inserts A, B, and C. The morphologic features in the mosaics compare well to the corresponding pathology of Fig. 3. As detailed in earlier reports<sup>9,10</sup> an exact correlation between features in the mosaics to those in the pathology is not expected because the H&E preparation is from the cut adjacent to the section imaged by the confocal microscope (Fig. 2). Further, the tissue sections are pliant and are inevitably distorted during fixing for mosaicing and hematoxylin and eosin (H&E) preparation.

Our results demonstrate that strip mosaicing is three times as fast as the previously reported two-dimensional mosaicing method with square images. Starting the merging process as the strips are acquired through the integration of the acquisition and merging programs will further reduce the turnaround time to produce mosaics. This, together with more precise stages, will allow us to generate  $10\times 10\ \text{mm}^2$  mosaics in less than the 3.1 min reported here. The projected acquisition time for a  $20\times 20\ \text{mm}^2$  mosaic would be 3.5 min and we anticipate a linear increase of acquisition time with sample area.

### Acknowledgments

The authors gratefully acknowledge support from NIH Grant No. R01EB012466 from NIBIB's Image Guided Interventions Program (Program Director Dr. John Haller). We thank Dr. Kishwer Nehal and Dr. Erica Lee for supplying discarded tissue from Mohs surgery (under an IRB-approved protocol), and William Fox, Scott Grodevant, and Zachary Eastman at Lucid Inc. for technical support.

### References

1. M. Rajadhyaksha, G. Menaker, T. Flotte, P. J. Dwyer, and S. Gonzalez, "Confocal examination of nonmelanoma cancers in thick skin excisions to potentially guide mohs micrographic surgery without frozen histopathology," *J. Invest. Dermatol.* **117**(5), 1137–1143 (2001).
2. R. Haque, R. Contreras, M. P. McNicoll, E. C. Eckberg, and D. B. Petitti, "Surgical margins and survival after head and neck cancer surgery," *BMC Ear Nose Throat Disord* **6**(2) (2006).
3. L. Jacobs, "Positive margins: The challenge continues for breast surgeons," *Ann. Surg. Oncol.* **15**(5), 1271–1272 (2008).
4. A. N. Yaroslavsky, J. Barbosa, V. Neel, C. DiMarzio, and R. R. Anderson, "Combining multispectral polarized light imaging and confocal microscopy for localization of nonmelanoma skin cancer," *J. Biomed. Opt.* **10**(1), 014011 (2005).
5. Z. Tannous, A. Torres and S. Gonzalez, "In vivo real-time confocal reflectance microscopy: A noninvasive guide for mohs micrographic surgery facilitated by aluminum chloride, an excellent contrast enhancer," *Dermatol. Surg.* **29**(8), 839–846 (2003).
6. A. Scope, U. Mahmood, D. S. Gareau, M. Kenkre, J. A. Lieb, K. S. Nehal, and M. Rajadhyaksha, "In vivo reflectance confocal microscopy of shave biopsy wounds: feasibility of intraoperative mapping of cancer margins," *Br. J. Dermatol.* **163**(6), 1218–1228 (2010).
7. V. Becker, T. Vercauteren, C. H. von Weyhern, C. Prinz, R. M. Schmid, and A. Meining, "High-resolution miniprobe-based confocal microscopy in combination with video mosaicing (with video)," *Gastrointest. Endosc.* **66**, 1001–1007 (2007).
8. K. E. Loewke, D. B. Camarillo, C. A. Jobst, and J. K. Salisbury, "Real-time image mosaicing for medical applications," *Studies in Health Technology and Informatics* **125**, 304–309 (2007).
9. J. K. Karen, D. S. Gareau, S. W. Dusza, M. Tudisco, M. Rajadhyaksha, and K. S. Nehal, "Detection of basal cell carcinomas in Mohs excisions with fluorescence confocal mosaicing microscopy," *Br. J. Dermatol.* **160**(6), 1242–1250 (2009).
10. D. S. Gareau, J. K. Karen, S. W. Dusza, M. Tudisco, K. S. Nehal, and M. Rajadhyaksha, "Sensitivity and specificity for detecting basal cell carcinomas in Mohs excisions with confocal fluorescence mosaicing microscopy," *J. Biomed. Opt.* **14**(3), 034012 (2009).
11. D. S. Gareau, Y. B. Li, B. Huang, Z. Eastman, K. S. Nehal, and M. Rajadhyaksha, "Confocal mosaicing microscopy in Mohs skin excisions: feasibility of rapid surgical pathology," *J. Biomed. Opt.* **13**(5), 054001 (2008).
12. P. Thevenaz and M. Unser, "User-friendly semiautomated assembly of accurate image mosaics in microscopy," *Microsc. Res. Tech.* **70**(2), 135–146 (2007).